FAILURE MODELING OF A SELF PIERCING RIVETED JOINT USING LS-DYNA

Silke Sommer[*], Johannes Maier[**]

[*]Fraunhofer Institute for Mechanics of Materials IWM
Woehlerstrasse 11, 79108 Freiburg, Germany
Email: silke.sommer@iwm.fraunhofer.de

[**]LuK GmbH & Co. KG
Industriestr. 3, 77815 Bühl, Germany

Abstract

Besides the basic product requirements, the aspect of energy efficiency is in the center of automobile engineering. A mixture of different light weight materials like aluminium and higher strength steels, called multi-material mix, is used increasingly to fulfill these requirements and reduce the weight of the vehicles. Hence the challenges for the joining technique are increasing. Mechanical joining techniques like self piercing riveting have great potential to fulfill this challenge. In particular the joints are the highest loaded parts during crash loading and overloading situations and have to be modeled in crash simulations. Joints are modeled with simplified elements in crash simulations due to efficiency. The simplified models should be able to reproduce the deformation and failure behavior as well as the energy absorption of the joints with less computational cost but with adequate accuracy.

In this paper the modeling possibilities in LS-Dyna are investigated for a self piercing riveted joint of aluminium sheets. Beams, eight-noded hexahedrons, hexahedron clusters and constrained elements have been used for a simplified modeling of the riveted connection. The material models MAT_SPOTWELD, MAT_SPOTWELD_DAIMLER, MAT_ARUP_ADHESIVE, MAT_COHESIVE_MIXED_MODE_ELASTOPLASTIC_RATE and the constrained models CONSTRAINED_SPR2 and _SPR3 have been tested with the simplified rivet model. The failure models are based on forces and moments, on normal, shear and bending stresses, on stresses and fracture energies and on forces and displacements for the constrained SPR models. The model parameters were determined by simulation of specimen tests under tension, lap-shear, peel and combined loading and by fitting the measured force vs. displacement curves. The different numerical results are compared concerning the measured load bearing capacities and energy absorption. The comparison showed that the hexahedron element with MAT_COHESIVE_MIXED_MODE_ELASTOPLASTIC is the most promising model for self piercing riveted joints in aluminium sheets because of the good description of the measured force vs. displacement curves and energy absorption under tension and lap-shear loading. The weakness of this model is the insufficient modeling of the peel loading and the lack of a possibility to control mixed mode loading. The paper gives a recommendation for further developments of modeling self piercing riveted joints.

Keywords

Self piercing rivet, modeling of joints, simplified modeling, crash simulation

1. Introduction

Besides the basic product requirements on functionality, reliability and also design the aspects of environmental compatibility, energy efficiency and emission reduction are in the center of automobile engineering. A mixture of different light weight materials like aluminium, magnesium, composite materials and higher strength steels, called multi-material mix, is used increasingly to fulfill these requirements and reduce the weight of the vehicles. This results in reduction of fuel consumption and therefore lower carbon dioxide emissions. Hence the challenges for the joining technique are increasing while combining the single components of different materials to the load bearing body in white. Mechanical joining techniques are increasingly used in order to fulfill this challenge. The mechanical joining technique has the advantage to make mixed connections stable and reliable, without decreasing the material properties through thermal influences. Therefore a lot of mechanical joining techniques like self piercing riveting and screwing are used in the automobile production besides the conventional spot welding technique. In the last years the potential of these two mechanical joining techniques has been developed continuously.

In particular the joints are the highest loaded parts during crash loading and overloading situations. Crash simulations of whole vehicles are of main interest during the vehicle development process. The load bearing capacity of a body in white is mainly influenced by the joints. Connected areas in crash simulations are modeled with simplified elements, because detailed modeling with solid elements for the sheets and the joint is not applicable due to efficiency. The simplified models should be able to reproduce the deformation and failure behavior as well as the energy absorption of the joints with less computational cost but with adequate accuracy.

2. Characterization of the self piercing riveted joints

The modeling possibilities in LS-DYNA for riveted joints are in the focus of these investigations. The modeled connections contain two aluminium sheets of different sheet thicknesses and self piercing rivets of the manufacturer Böllhoff.

Figure 1 shows cuts through the three different riveted connections of the aluminium sheets made of the alloy AlMg0.8Si0.9 with equal sheet thicknesses of 2 mm and 1.2 mm and the combination of both sheet thicknesses. The self piercing rivets are C 5X4,5 SKR H4 and C 5X4 SKR H4, respectively.

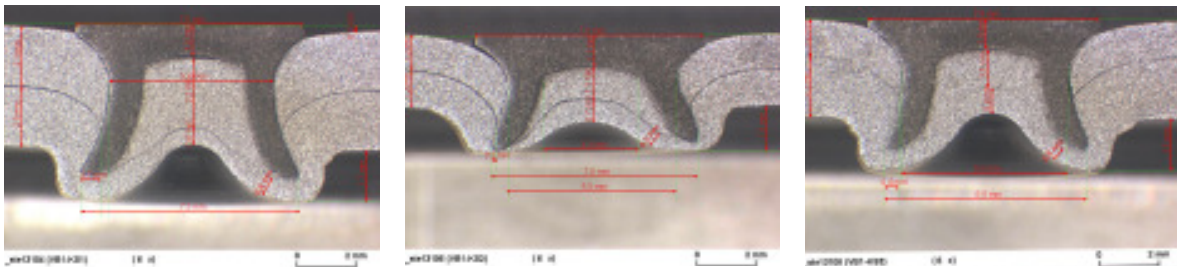

(a) (b) (c)

Figure 1: Cross sections of the untested self piercing riveted connections of equal sheet thicknesses of 2 mm (a) and 1.2 mm (b) and of the sheet thickness combination of 1.2 mm and 2 mm (c).

A variety of tests at different loading conditions under tension, shear and bending as well as combined tension-shear loading has been performed to characterize the deformation and failure behavior of these riveted connections. The specimen production and the experiments were conducted by the Laboratory for Materials and Joining Technology (LWF) of the University of Paderborn. The riveted specimens have been tested under the loading angles of 0°, 30°, 60° und 90° using the KS2 test set up [HAH95] shown in Figure 2 (b). Here, KS2-0° means shear loading and KS2-90° means tension loading. The used specimen geometry is shown in Figure 2 (a). The U-shaped halves of a specimen are assembled in the middle of the specimen with the self piercing rivet. The coach peel specimen is realized with two L-shaped sheets for bending loading on the riveted joint (Figure 2 (a)).

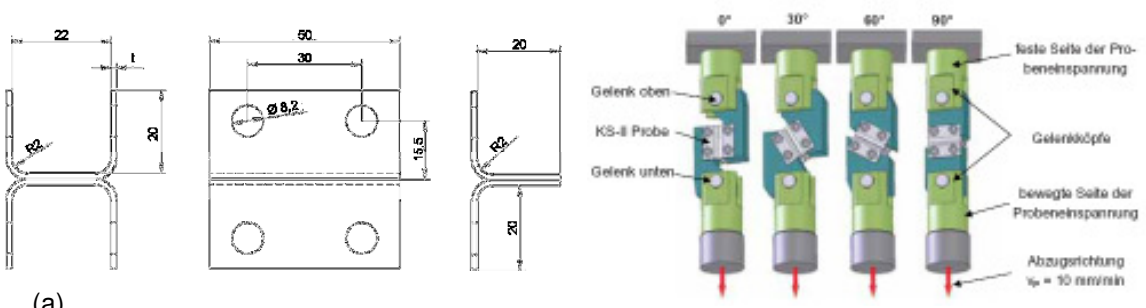

(a) (b)

Figure 2: Specimen geometries (a) and KS2 test set up (b) [WIS08].

The measured load vs. displacement curves of the riveted assembly of the 2 mm thick sheets are shown in Figure 3 (a). Five repeat tests were conducted for each loading direction marked in the same colour. Figure 3 (b) shows the maximal and minimal failure curves. These curves are derived of the measured maximal and minimal load bearing capacities, which are divided in normal and shear force according to the corresponding loading angles.

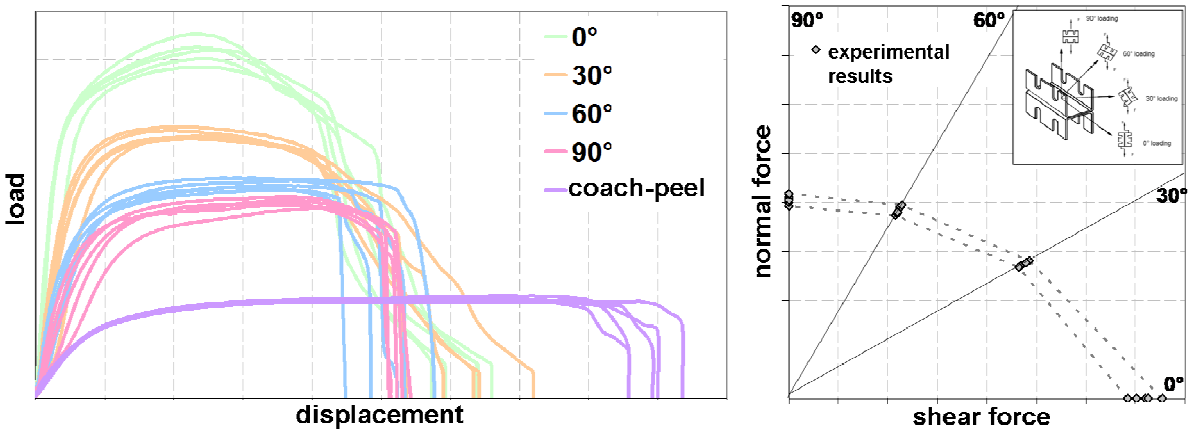

(a) (b)

Figure 3: Measured load vs. displacement curves of the riveted assembly of the 2 mm thick sheets (a) and maximal and minimal failure curves (b).

The measured load vs. displacement curves of the riveted connections of the three different sheet thickness combinations are shown in Figure 4 for shear (0°), tension (90°) and peel loading.

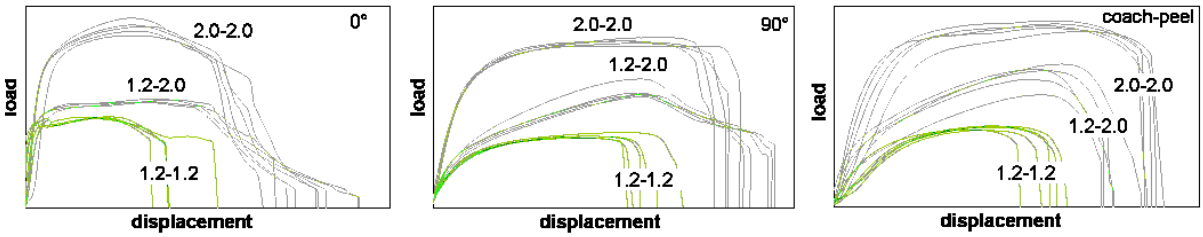

(a) (b) (c)

Figure 4: Measured load vs. displacement curves of shear loading (a), tension loading (b) and peel loading (c) for the riveted joint of AlMg0.8Si0.9 sheets with the thicknesses 2.0 mm-2.0 mm, 1.2 mm-2.0 mm and 1.2 mm-1.2 mm.

3. Modeling of the self piercing riveted joints

The self piercing riveted joints are built up with different geometrical models and material models to describe the observed deformation and failure behavior of the mechanical joints due to shear, tension and peel loading. First, the modeling of the riveted connection of the 2 mm thick sheets is shown.

3.1. Modeling of rivet, specimen and test set up

The modeling of the test set up for tension loading (KS2-90°) including the specimen and the rivet is described in Figure 5. The sheets are modelled with shell elements. The shell element edge length is 2.5 mm in the deformable, free parts of the specimen. The material model MAT_PIECEWISE_LINEAR_ PLASTICITY (MAT_024) [LSD10] with the measured true stress vs. true strain curve of the aluminium alloy and without failure modeling for the sheets is used for the deformable shell parts.

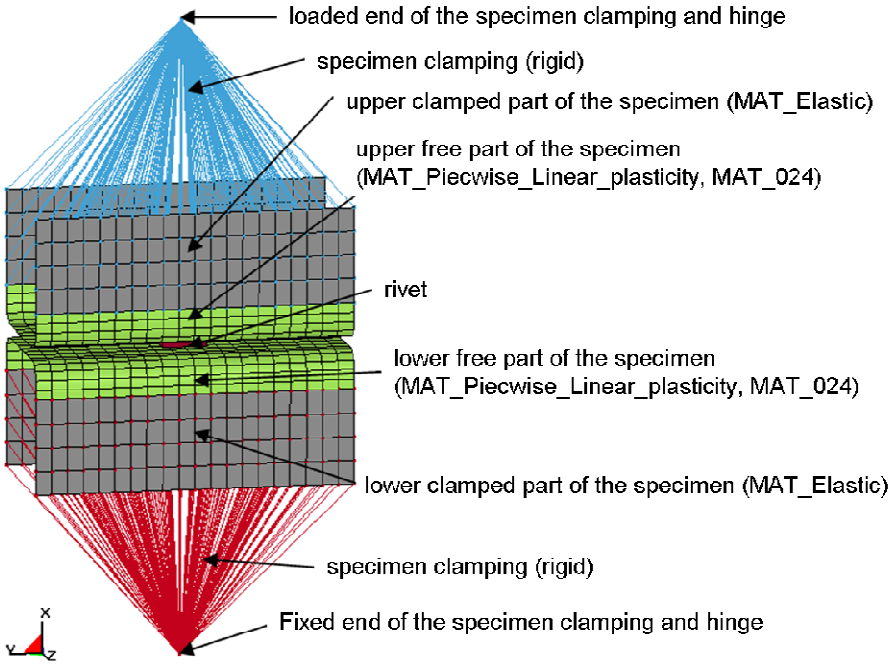

Figure 5: Finite element model for the specimen and the test set up for tension (KS2-90°) loading

The different models for the rivet are shown in Figure 6. First, a beam element is used, which is shown in Figure 6 (a). The length is chosen according to the thicknesses of the sheets. The diameter of the beam is 7.75 mm. The connection to the shell elements is realized through the contact option CONTACT_SPOTWELD. In Figure 6 (b) the hexahedron spot weld model is shown. An eight-noded, underintegrated solid element is used. The quadratic bottom surface corresponds to the cross section of the riveted connection with the diameter 7.75 mm. The width of the element is 6.9 mm and the height 2.0 mm resulting from the sheet thicknesses. The connection to the shell elements is realized through the contact option CONTACT_TIED_SURFACE_TO_SURFACE. The hexahedron cluster (Figure 6 (c) consists of four eight-noded, underintegrated solid elements with a hexagonal cross section. The outer nodes of the cluster are positioned on the circumference of the rivet. This results in 90% of the cross section area of the riveted connection. Again, the contact option CONTACT_TIED_SURFACE_TO_SURFACE is chosen to join the cluster elements to the shell elements.

The Constrained Self Piercing rivet model (CONSTRAINED_SPR) is shown in Figure 6 (d). The diameter of the domain of influence and a rivet node position are defining the connection model as shown in Figure 7. The rivet node is positioned in the middle between both sheets. The nodes of the shell elements, which are connecting the two sheets through constrained conditions, are determined through an orthogonal projection of the domain of influence with diameter of 7.75 mm for this riveted connection to the shell elements [DYN10].

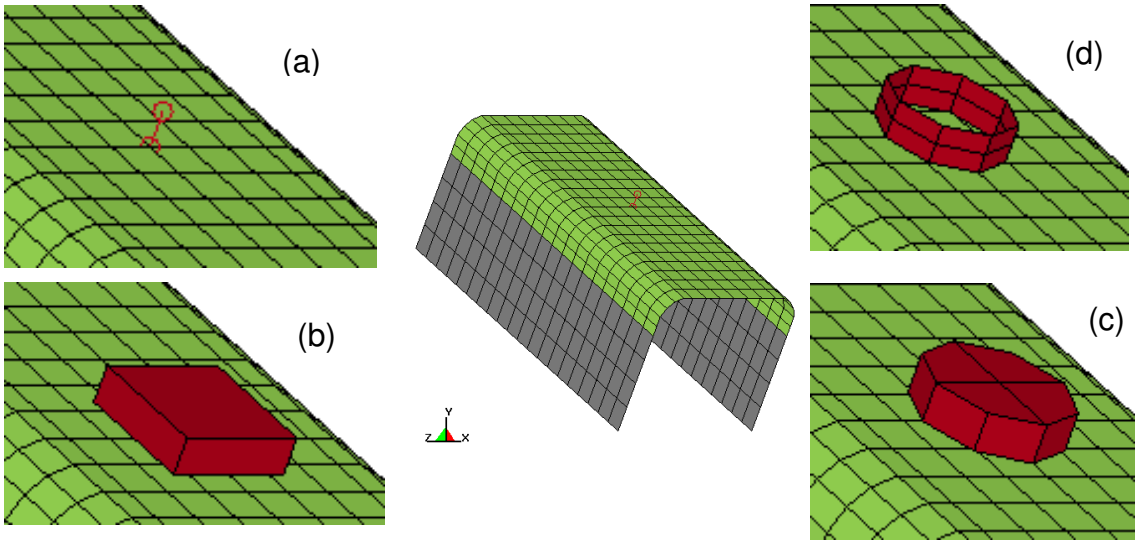

Figure 6: Finite element model of a half of the specimen and different simplified models for the rivet: (a) beam element, (b) hexahedron element, (c) constrained element, (d) cluster of four hexahedron elements.

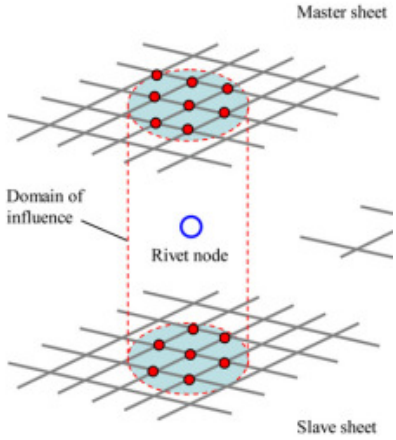

Figure 7: Diameter of the domain of influence and rivet node position for definition of CONSTRAINED_SPR2

3.2. Material models

In this section the used material models for the riveted connection are introduced. These are the elastic-plastic material models, constrained models and cohesive material models.

3.2.1. MAT_SPOTWELD_DAMAGE-FAILURE (MAT_100)

MAT_SPOTWELD is used for beam and solid elements to model the rivet. The hexahedron element is a one point integrated solid used with the Belytschko-Bindemann hourglass control. The plasticity model is an elastic-plastic von Mises formulation with a bi-linear hardening. A force and moment based failure criteria

Fehler! Es ist nicht möglich, durch die Bearbeitung von Feldfunktionen Objekte zu erstellen. (1)

is used. f_n and f_s are the actual normal force and shear force, respectively. m_b and m_t are the bending and torsion moment, respectively. The corresponding variables in capital letters are the critical values, which have to be determined. If equation (1) is fulfilled, the hexahedron is eliminated immediately.

3.2.2. MAT_SPOTWELD_DAIMLER (MAT_100_DA)

MAT_SPOTWELD_DAIMLER is an enhancement of MAT_100 of the Daimler AG [SEE05]. The damage and failure model is based on stresses. Different damage types are available for modeling damage initiation and damage development. The failure function

$$f = \left(\frac{\sigma_n}{D\_SN}\right)^{D\_EXSN} + \left(\frac{\sigma_b}{D\_SB}\right)^{D\_EXSB} + \left(\frac{\tau}{D\_SS}\right)^{D\_EXSS} - 1 \quad (2)$$

is a power law combination of the normal stress σ_n, the bending stress σ_b and the shear stress τ. The failure parameters are the critical normal stress D_SN, the critical shear stress D_SS and the critical bending stress D_SB und the interaction exponents D_EXSN, D_EXSB and D_EXSS. The failure parameters are defined on the card DEFINE_CONNECTIONS_PROPERTIES.

If damage type (DG-TYP) 0 is used, the hexahedron is eliminated when the failure function f is greater zero. Damage type (DG-TYP) equal 4 describes damage initiation and damage development. A linear decrease of stress with increasing strain after reaching the load bearing capacity is considered using the fracture energy G_{Fade} (Figure 8). Details of the different damage types are given in [HAU09].

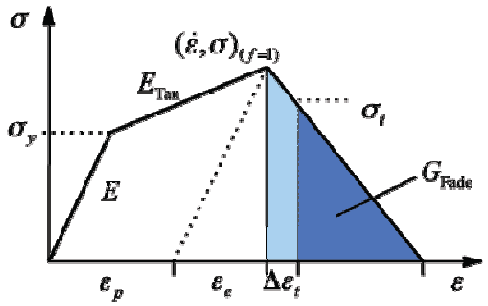

Figure 8: stress vs. strain characteristics of DG_TYP 4 with consideration of the fracture energy G_{Fade}

3.2.3. MAT_ARUP_ADHESIVE (MAT_169)

MAT_ARUP was implemented for modeling of adhesive bonding and is a cohesive zone model. The plasticity model is not volume-conserving and available only for solid elements. The yield condition and failure surface are treated as a power law combination of direct tension and shear (, used here as

$$\left(\frac{\sigma}{\sigma_{max}}\right)^{PWRT} + \left(\frac{\tau}{\tau_{max}}\right)^{PWRS} - 1 = 0. \quad (1)$$

σ is the actual normal stress, τ the actual shear stress, σ_{max} die critical normal stress, τ_{max} the critical shear stress and PWRT and PWRS the exponents of the interaction of shear and tension mode.

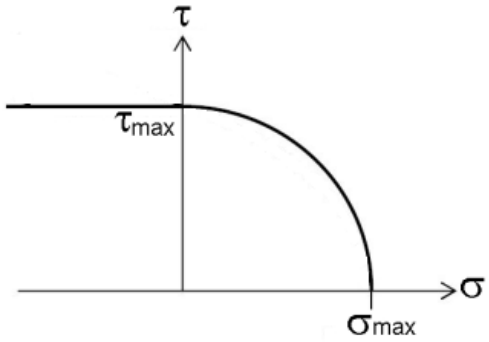

Figure 9: yield and failure surface of MAT_ARUP

Failure initiates, if the condition in equation (1) is true. The load bearing capacity is decreased linearly to zero with increasing displacement, that the fracture energy in mode I ($G_{C,ten}$) and mode II ($G_{C,shear}$) are reached as shown in Figure 10. $G_{C,ten}$ and $G_{C,shear}$ are also parameters of the model.

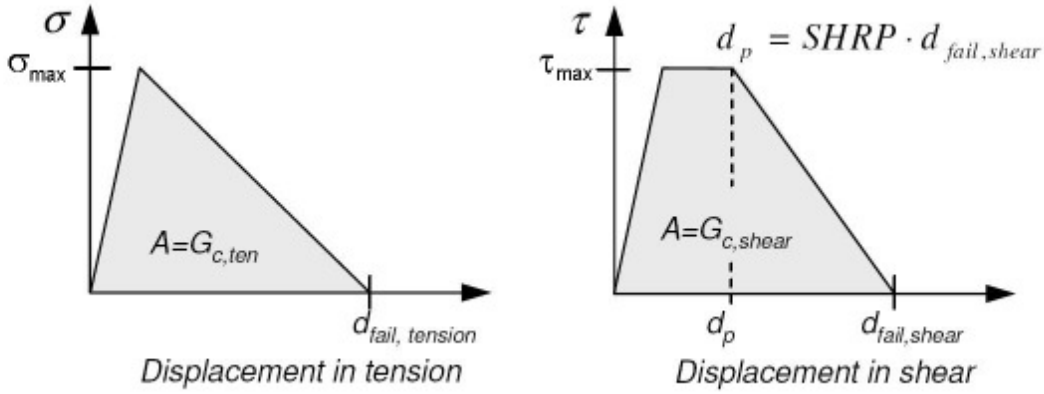

Figure 10: stress vs. displacement curves in tension (left) and shear (right) of the MAT_ARUP

3.2.4. MAT_COHESIVE_MIXED_MODE_ELASTOPLATIC_RATE (MAT_240)

The material model MAT_COHESIVE_MIXED_MODE_ELASTOPLATIC_RATE is also a cohesive formulation. It is a tri-linear elastic-ideally plastic cohesive zone model, which was developed by Marzi et al. [MAR09] for adhesive bonding. Figure 11 shows the trilinear single and mixed-mode traction vs. separation law. Details, equations and parameter definitions of this model are given in [MAR09, LSD10, MAR10].

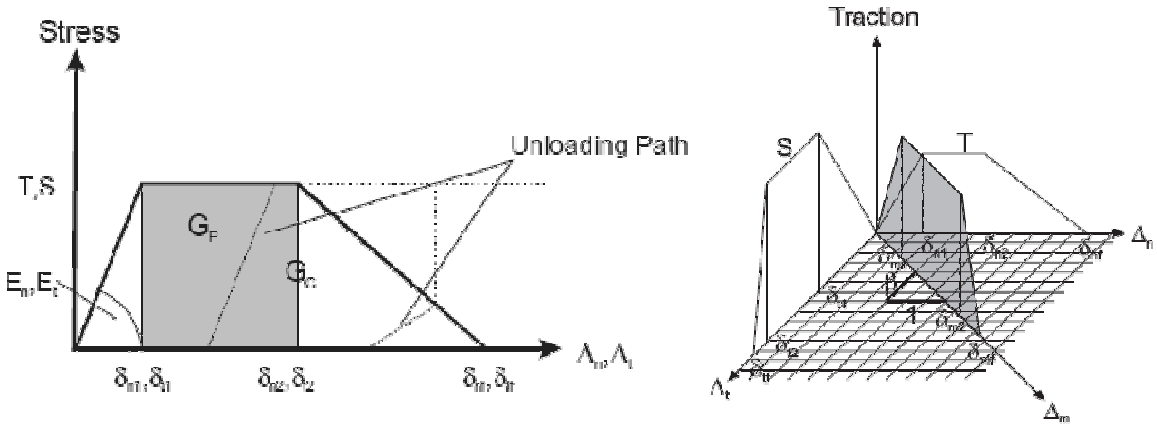

Figure 11: Trilinear traction-separation law for shear and tension stress (left) and mixed-mode traction-separation law (right)

3.2.5. CONSTRAINED_SPR2

The Constrained_SPR2 (self-piercing rivet) model was developed and implemented by Hanssen, Porcaro et al. [HAN10], [POR08] at SIMLab in Trondheim. This model was explicitly developed for modeling self piercing riveted joints of aluminium sheets.

The normalized normal force f_n / f^{max}_n and shear force f_t / f^{max}_t in dependence of normalized displacements are calculated under pure tension and pure shear according to the equations given in [HAN10, LSD10] and are shown in Figure 12. f^{max}_n and f^{max}_t are the maximum normal and shear loads, respectively. For mixed-mode behavior an effective displacement and force are calculated by an angle dependent term and a damage dependent term. The parameter THICK specifies the distance between the upper and lower sheet, and the rivet node specifies the position of the rivet.

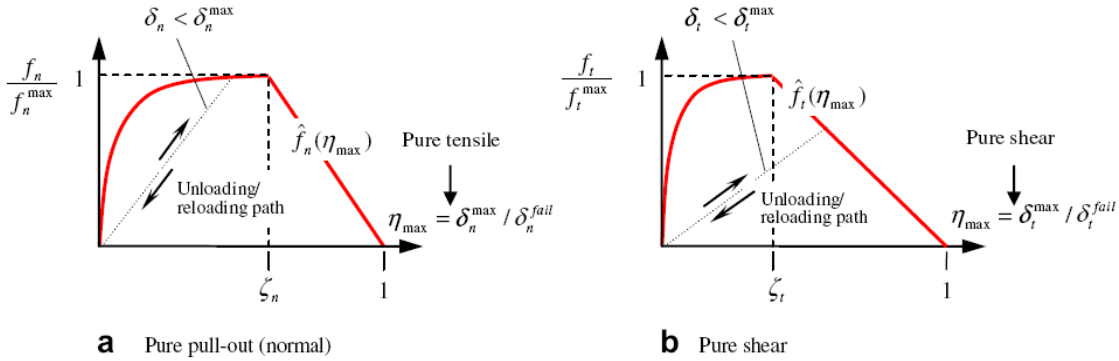

Figure 12: force vs. displacements curves for pure tension (a) and pure shear (b)

4. Results

The tested combinations of geometrical models and material and failure models are listed in Table 1. Only a selection of the calculated force vs. displacement curves are presented in the following and compared to the measured curves.

No.	Geometry	Material model	MAT No.
1	Beam	MAT_SPOTWELD_DAMAGE-FAILURE	MAT_100
2	Hexahedron	MAT_SPOTWELD_DAMAGE-FAILURE	MAT_100
3		MAT_SPOTWELD_DAIMLER / Damage-Typ 0	MAT_100_DA (DG-TYP 0)
4		MAT_SPOTWELD_DAIMLER / Damage-Typ 4	MAT_100_DA (DG-TYP 4)
5		MAT_ARUP_ADHESIVE	MAT_169
6		MAT_COHESIVE_MIXED_MODE_ ELASTOPLASTIC_RATE	MAT_240
7	Hexahedron-Cluster (without assembly)	MAT_SPOTWELD_DAMAGE-FAILURE	MAT_100
8		MAT_SPOTWELD_DAIMLER / Damage-Typ 0	MAT_100_DA (DG-TYP 0)
9		MAT_SPOTWELD_DAIMLER / Damage-Typ 4	MAT_100_DA (DG-TYP 4)
10		MAT_ARUP_ADHESIVE	MAT_169
11		MAT_COHESIVE_MIXED_MODE_ ELASTOPLASTIC_RATE	MAT_240
12	Hexahedron-Cluster (with assembly)	MAT_SPOTWELD_DAIMLER / Damage-Typ 0	MAT_100_DA (DG-TYP 0)
13		MAT_SPOTWELD_DAIMLER / Damage-Typ 4	MAT_100_DA (DG-TYP 4)
14	Beam-Hexahedron-Cluster	MAT_COHESIVE_MIXED_MODE_ ELASTOPLASTIC_RATE	MAT_240
15	Constrained_SPR	CONSTRAINED_SPR2	
16		CONSTRAINED_SPR3	

Table 1: Tested combinations of rivet, material and failure models

The result of the different material models usable for hexahedron elements are shown in Figure 13 for the three loading case 0° (shear), 90° (tension) and peel (bending) load. Also different failure models are used. The material models MAT_100 and MAT_100 DS with DG-TYP 0 results in a failure of the hexahedron at force maximum. All other material models are describing failure initiation and development. They are taking into account the degradation of the load after the load bearing capacity is reached.

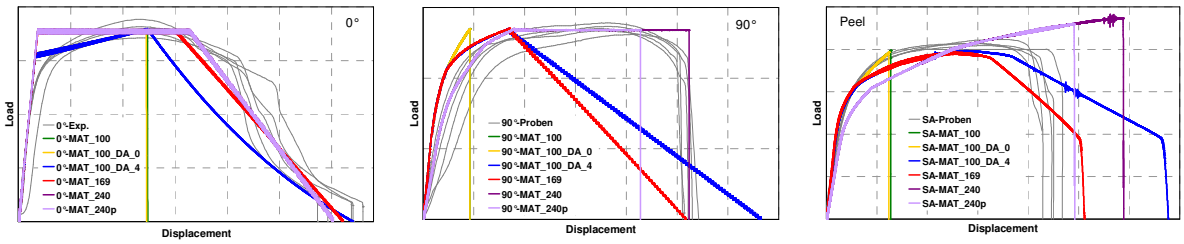

(a) (b) (c)

Figure 13: Comparison of measured and calculated force vs. displacement curves using hexahedron elements and different material models

Figure 14 shows the comparison of the most promising modeling techniques for the riveted joint of the 2.0 mm thick aluminium sheets. The shear loading at 0° is well depicted of all chosen material models. Differences are visible in the 90° and peel loading. The model MAT_240p HEX is an optimized parameter set, so describe both loading cases - 90° and the peel load - with less deviation.

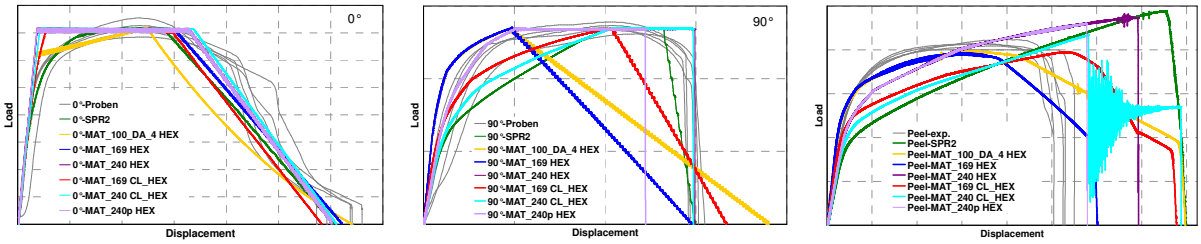

Figure 14: Comparison of measured and calculated force vs. displacement curves using hexahedron elements and hexahedron clusters and different material models

Figure 15, Figure 16 and Figure 17 are showing the comparison for all tested loading situations between the experiments and the hexahedron element with MAT_240 for the three investigated connections with the sheet thicknesses 2.0 mm, 1.2 mm and the unequal connection of 1.2 mm and 2.0 mm sheet thicknesses.

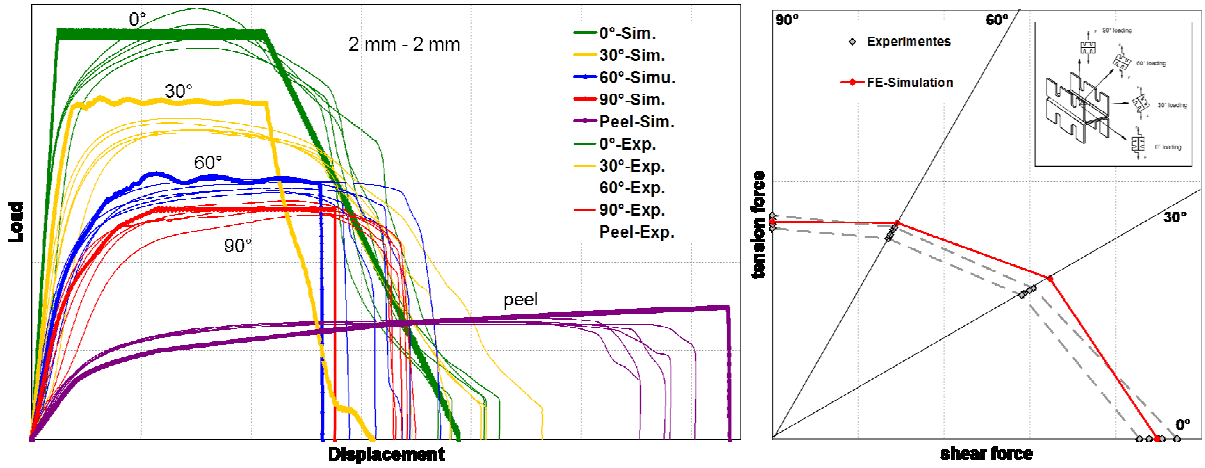

Figure 15: Comparison of measured and calculated force vs. displacement curves using one hexahedron and and MAT_240 for different loading situations (left) and failure curve diagram (right) for the riveted joint in 2 mm thick aluminium sheets

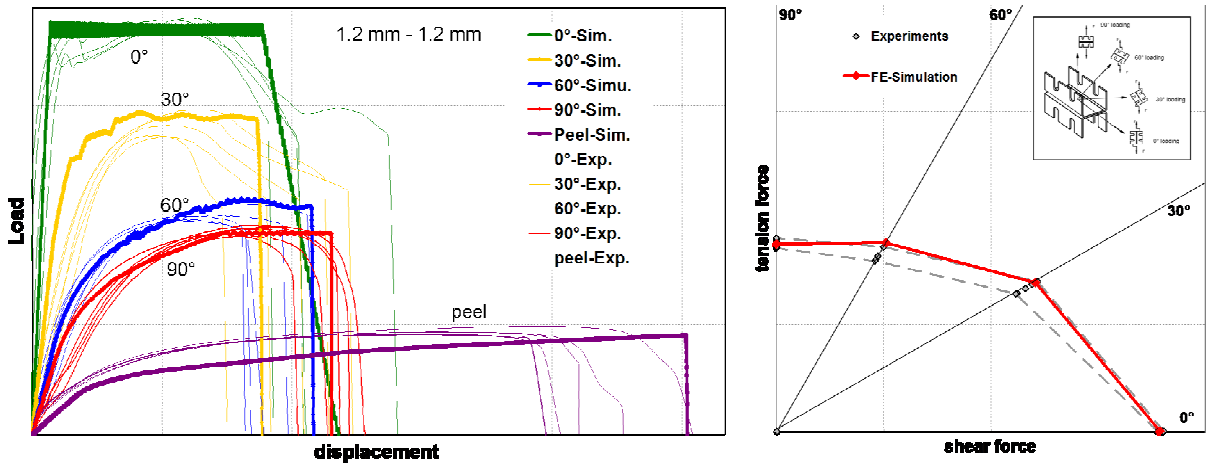

Figure 16: Comparison of measured and calculated force vs. displacement curves using one hexahedron and and MAT_240 for different loading situations (left) and failure curve diagram (right) for the riveted joint in 1.2 mm thick aluminium sheets

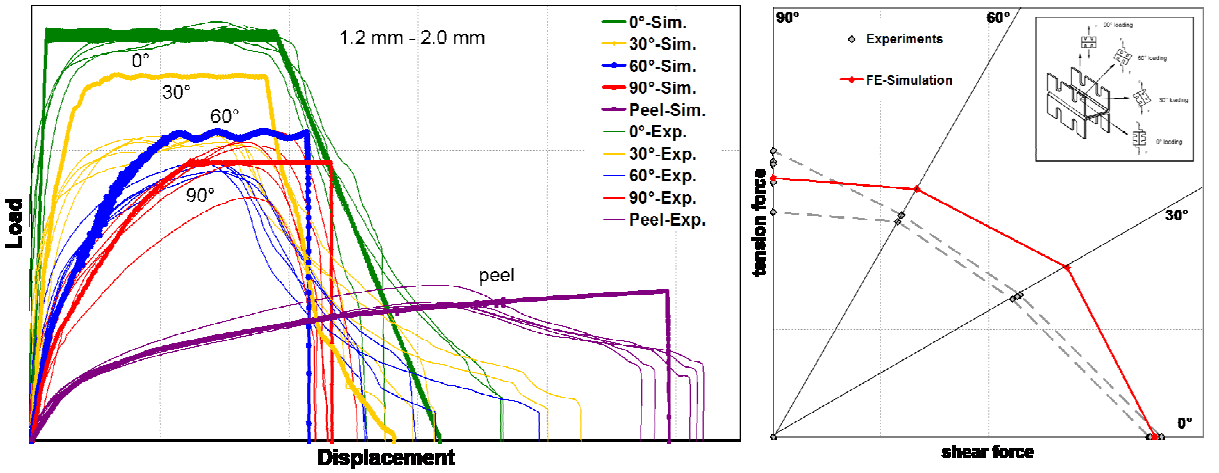

Figure 17: Comparison of measured and calculated force vs. displacement curves using one hexahedron and MAT_240 for different loading situations (left) and failure curve diagram (right) for the riveted joint of unequal sheet thicknesses 1.2 - 2.0 mm

5. Conclusions and summary

The possibilities of modeling self piercing riveted joints with LS-DYNA are investigated in this paper. Different simplified modeling techniques are investigated with regard to model the measured load bearing capacity and energy absorption. The different geometrical models beam elements, hexahedron elements, hexahedron-clusters and constrained elements are used. MAT_SPOTWELD (MAT_100), MAT_SPOTWELD_DAIMLER (MAT_100_DA) Damage (DG)-Typ 0 and 4, MAT_ARUP_ADHESIVE (MAT_169), MAT_COHESIVE_MIXED_MODE_ELASTOPLASTIC_ RATE (MAT_240) and the constrained models CONSTRAINED_SPR2 und CONSTRAINED _SPR3 have been used as material models. Altogether 16 different combinations of geometrical, material and failure models have been investigated.

The model parameters are determined by fitting the measured force vs. displacement curves. The most promising models are compared finally. The beam element is not a promising model because of the high rotations under shear loading. That is the reason, why it was not possible to calibrate a set of parameters for shear and tension loading. The parameters of the CONSTRAINED_SPR2 model are easy to calibrate, also the model parameters of MAT_100_DA DG-TYP 4, MAT_169 und MAT_240 are well fittable to the measured force vs. displacement curves. The MAT_100 and MAT_100_DA DG-TYP 0 are excluded, because the modeling of the decreasing of load bearing after force maximum is not possible and therefore the energy absorption is underestimated. The hexahedron-cluster with the assembly function is not implemented yet with MAT_100_DA DG-TYP 4, MAT_169 und MAT_240.

In this comparison the material model MAT_COHESIVE_MIXED_MODE_ELASTOPLATIC_RATE (MAT_240) with one hexahedron element is the most promising model to describe the deformation and failure behavior of the riveted joint. The weakness of this model is the lack of a parameter for calibration of the interaction between shear and tension loading and the difficulties to describe tension and bending with the same accuracy. MAT_240 was also used to model two more riveted connections with different sheet thicknesses (1.2 mm to 1.2 mm and 1.2 mm to 2.0 mm) with a high accuracy.

In the ongoing investigation self piercing riveted joints of aluminium and steel sheets will be tested and modeled. Also higher loading velocities and the dependence of the load bearing capacities and energy absorption on the strain rate will be in the focus of the investigations. For validation of the modeling technique crash tests with components will be conducted and simulated.

6. Acknowledgements

This work has been funded with budget funds of the Federal Ministry of Economics and Technology (BMWi) via the German Federation of Industrial Research Associations „Otto von Guericke“ e.V. (AiF) (IGF-Nr. 352 ZBG) and supported by the Forschungsvereinigung Stahlanwendung e.V. FOSTA, Sohnstrasse 65, 40237 Duesseldorf (Research Association for Steel Application). The authors would like to thank all parties involved for the funding and the support.

7. Literature

[HAH95] Prof. Dr.-Ing. O. Hahn, Patentnummer DE 195 22 247 A1, Probe und Probespann-vorrichtung zum Einsatz in Zugprüfmaschinen, Paderborn, 1995

[WIS08] M. P. Wißling, O. Hahn, Methodenentwicklung zur Auslegung mechanisch gefügter Verbindungen unter Crashbelastung, Band 78 / D 466 (Dissertation Universität Paderborn), Shaker Verlag, Aachen, 2008

[LSD10] LS-DYNA Keyword User's Manual Volume 1 and 2, Version 971/Rev 5 (beta), Livermore Software Technology Corparation (LSTC), Livemore (USA), 2010

[HAN10] A.G. Hanssen, L. Olovsson, R. Porcaro, M. Langseth, A large-scale finite element point-connector model for self-piercing rivet connections, European Journal of Mechanics A/Solids 29 S.484-495, Trondheim (Norway), 2010

[POR08] R. Porcaro, M. Langseth, L. Olovsson, A.G. Hanssen, Behaviour and modelling of self-piercing rivet connections, IMPACT LOADING OF LIGHTWEIGHT STRUCTURES, SIMLab, Trondheim (Norway), 2008

[SEE05] F. Seeger, M. Feucht, Th. Frank, B. Keding, A. Haufe, An investigation on spot weld modeling for crash simulation with LS-DYNA, proceedings 4th LS-DYNA Anwenderforum, Bamberg, 2005

[HAU09] A. Haufe, T. Graf, G. Pietsch, M. Feucht, F. Neukamm, Aktuelle Trends bei der Modellierung von Schweißpunktverbindungen in der Crash-Simulation mit LS-DYNA, Proceedings crashMAT, Freiburg, 2009

[MAR09] S. Marzi, O. hesebeck, M. Brede, F. Kleiner, A Rate-dependent, Elasto-plastic Cohesive Zone Model for crash Analysiy of Adhesively Bonded Joints, proceeding 7th European LS-DYNA Conference, Salzburg, 2009

[MAR10] S. Marzi, Ein ratenabhängiges, elasto-plastisches Kohäsivzonenmodell zur Berechnung struktureller Klebverbindungen unter Crashbeanspruchung, Dissertation, Aachen, 2010